Chinese Chemical Letters 33 (2022) 4229–4232

Contents lists available at ScienceDirect

Chinese Chemical Letters

journal homepage: www.elsevier.com/locate/cclet

Lysosome-targeting red fluorescent probe for broad carboxylesterases detection in breast cancer cells

Yanyan Sun[a,1], Xiaonan Zhou[b,1], Liyuan Sun[a], Xiuxiu Zhao[a], Yongrui He[a], Ge Gao[a,*], Weina Han[a], Jin Zhou[a,*]

[a] School of Pharmacy, School of Rehabilitation Medicine, Weifang Medical University, Weifang 261053, China
[b] Weifang Maternal and Child Health Hospital, Maternal and Child Health Hospital of Weifang Medical University, Weifang 261011, China

ARTICLE INFO

Article history:
Received 21 October 2021
Revised 27 January 2022
Accepted 29 January 2022
Available online 4 February 2022

Keywords:
Fluorescent probe
Carboxylesterases
Broad detection
Breast cancer
Lysosome-targeting
Red fluorescence

ABSTRACT

Available online The abnormal carboxylesterase (CES) expression is closely related to many diseases such as hyperlipidemia, atherosclerosis, obesity, liver cancer, type 2 diabetes mellitus and gastrointestinal stromal tumors. The detection of a single enzyme in practical samples is often constrained by the structural diversity of CESs. Thus, the development of broad-carboxylesterase responsive fluorescent probe, which can detect the presence of wide variety of CESs, may provide overall or category information from another point of view, supplementing the deficiency of single detection for CES subspecies. Organelle lysosome is involved in various cell processes, such as cell signaling, apoptosis, secretion, and energy metabolism. Up to date, lysosome-targeted fluorescent probes, especially those with red emission (over 550 nm, with relatively low biological harmfulness), for CES detection are still rare. A lysosomes-targeted red fluorescent probe CES-Lyso was designed to monitor intracellular a variety of carboxylesterases alteration with wonderful selectivity and sensitivity, which was further applied to distinguish different derived breast cancer cells and monitor carboxylesterase activity in the anticancer drug treatment.

Carboxylesterase (CES, with EC 3.1.1.1), a kind of serine hydrolase, is widely distributed throughout the body and exhibits broad substrate specificity such as esters, amides, thioesters, and carbamates which are involved in xenobiotic and endobiotic metabolism [1,2]. As a phase I metabolic enzyme, CES participates not only in the disintoxication of pesticides and environmental toxins, but also in the biotransformation of many drugs. Because its active sites could irreversibly bind with related drug, CES is considered to be a pivotal drug target and pre-drug trigger [3]. The abnormal CES expression is closely related to many diseases such as hyperlipidemia, atherosclerosis, obesity, liver cancer, type 2 diabetes mellitus and gastrointestinal stromal tumors [4]. Five types of human CESs (CES1, CES2, CES3, CES4, and CES5) have been reported so far, based on their substrate specificity and basal regulation difference [5].

Fluorescent technique provides an excellent candidate method for the CES detection and related functional research owing to its advantages of high sensitivity, fast detection, high spatiotemporal resolution, simple operation and non-invasive ability in living systems, attracting great attention [6–11]. A handful of previous works have shown their fluorescent probes to selectively detect the specific CES, mainly CES1 [12–14] and CES2 [15–17]. Admittedly, their selective responses have significant advantages and positive significance. However, there are a variety of factors that cause interindividual difference of CES activity, which brings the variability of clinical outcomes [18]. Besides, the detection of a single enzyme in practical samples is often constrained by the structural diversity of CESs. Thus, the development of broad-carboxylesterases responsive fluorescent probe, which can detect the presence of wide variety of CESs, may provide overall or category information from another point of view, supplementing the deficiency of single detection for CES subspecies. Organelle lysosome is involved in various cell processes, such as cell signaling, apoptosis, secretion, and energy metabolism [19]. Up to date, lysosome-targeted fluorescent probes, especially those with red emission (over 550 nm, with relatively low biological harmfulness), for CES detection are still rare.

In this study, we put forward a new lysosome-targeted red fluorescent probe (CES-Lyso, Scheme 1) to sense a wide variety of CESs. Furthermore, CES-Lyso could be successfully applied for *in situ* visualization of CES activity in live cells. Additionally, CES-Lyso has

* Corresponding authors.
E-mail addresses: gaoge@wfmc.edu.cn (G. Gao), zhoujin@wfmc.edu.cn (J. Zhou).
[1] These authors contributed equally to this work.

https://doi.org/10.1016/j.cclet.2022.01.087
1001-8417/

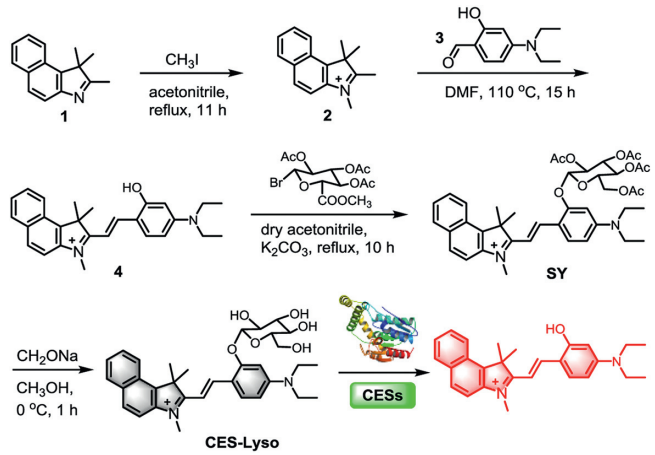

Scheme 1. The chemical synthesis and suggested mechanism of probe CES-Lyso for CES response.

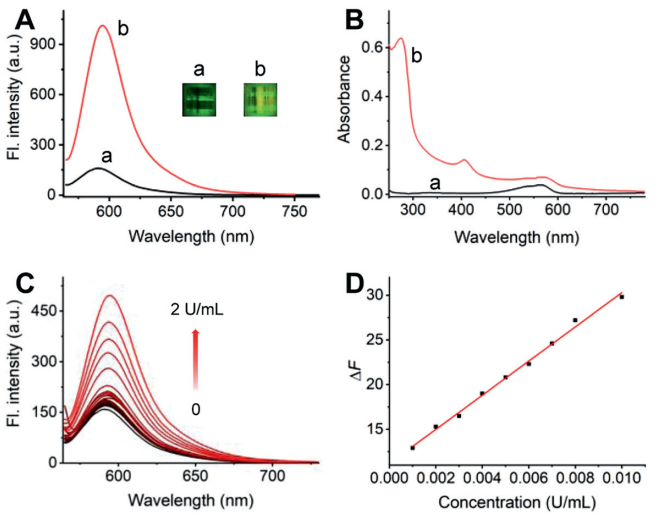

Fig. 1. Fluorescence emission (A) and adsorption (B) spectral response of CES-Lyso (10 μmol/L) before (a) and after (b) the addition of 5 U/mL CES in the PBS of pH 7.4. Insets in panel A: the photoes of the corresponding visible fluorescence changes of aqueous CES-Lyso. (C) Fluorescence spectral changes of CES-Lyso (10 μmol/L) with the increase of CES concentration (0-2 U/mL). (D) The fitted linear relationship of the fluorescence intensity changes at the peak *versus* CES concentration. $\lambda_{ex/em}$ = 555/595 nm.

been successfully used to discriminate different derived breast cancer cells and monitor CES fluctuation in the anticancer drug treatment.

Hemicyanine-based fluorophores demonstrate high thermal stability and biocompatibility along with photophysical properties [20–22]. Herein, we first rationally designed a hemicyanine fluorophore **4** (Scheme 1) by a reliable condensation reaction between indoline 1,1,2,3-tetramethyl-1*H*-benzo[*e*]indol-3-ium (**2**) and 4-(diethylamino)-2-hydroxybenzaldehyde (**3**) in DMF. In essence, the designed presence of the cationic indoline moiety introduced desirable aqueous solubility. The water soluble diethylamino moiety also enhanced electron donating ability, redshiftting the emission wavelength. Then, a nucleophilic substitution reaction was taken between **4** and 2,3,4,6-tetraacetoxy-α-D-pyranose bromide to produce the key intermediate, **SY**, subsequently the following transesterification reaction afforded the final probe CES-Lyso with a glycosidic bond between carbohydrate and the fluorophore. The structures of CES-Lyso and its related intermediate products were confirmed by ^{1}H NMR, ^{13}C NMR, and highly resolutionized ESI-MS spectroscopy (Figs. S1-S9 in Supporting information).

Firstly, we evaluated the spectroscopic properties of the probe CES-Lyso towards CESs (Fig. 1, Fig. S10 in Supporting information). In the exploratory experiment stage, commercially available CES from porcine liver was used to carry out the test initially. As shown in Fig. 1A, after incubation with 5 U/mL CES, a remarkable fluorescence increasement could be detected with the emission peak at 595 nm under the excitation of 555 nm, and the obvious fluorescence color change could be observed in the inset of Fig. 1A. Meanwhile, the optimum absorption became blue shift from 563 nm to 275 nm (Fig. 1B). The results suggested that CES-Lyso is a typical off-on probe with red fluorescence for CES. Next, the influences of incubation time, temperature and pH on the reaction between CES-Lyso and CES with various concentrations (0, 2, 5, and 10 U/mL) were studied. As displayed in Fig. S10, the turn-on fluorescence could be triggered by CES instantly within several dozens of seconds, which possesses the advantage in rapid detection; the temperature-dependence investigation of CES-Lyso reacting with CES shows that the probe works most efficiently around 37 °C, though it has a certain spectral response under conditions deviating from physiological temperature; the important evaluation index pH examination shows that CES-Lyso reacts well with CES in a wide pH range environment from 4.1 to 9.9 in PBS (phosphate buffer). It can also be concluded that the probe itself keeps fluorescence stable in the above examinations of reaction time, wide temperature and pH range. These results suggest that CES-Lyso performs well for the CES quick response under complex physiological conditions (37 °C and around the neutral).

Under the artificial physiological conditions of medium with 37 °C and pH 7.4, the CES-Lyso (10 μmol/L) was mixed and incubated with CES in a series of concentrations for the quantitative purpose. The spectral titration experiment examination was performed to gain the sensitivity performance of CES-Lyso towards CES. As displayed in Fig. 1C, the fluorescence intensity of CES-Lyso increased as a function of raising the CES content, and the degree of fluorescence enhancement became slow when the concentration of CES-Lyso was more than 0.01 U/L. The fluorescence response of CES-Lyso exhibits an excellent linear trend to the CES when the CES concentration ranges from 1.0×10^{-3} to 1.0×10^{-2} U/L, with a function formula of $\Delta F = 1.91 \times 10^{3}$ C (U/mL) + 11.2 (Pearson's correlation coefficient $r = 0.997$), in which ΔF is the fluorescence enhanced value deducing the background fluorescence of CES-Lyso (Fig. 1D). With the reference of a previous method [23–27], the limit of detection (LOD) was tested to be as low as 6.07×10^{-4} U/L (around 45 ng/L) based on the calculation with 3*S*/*m*, where *S* is the standard deviation of 11 measurements of blank solution and *m* is the measured slope of the fitting curve. The results suggest that CES-Lyso is a promising probe for quantitatively detect CES with high sensitivity.

Then, the selective response of CES-Lyso towards various potential interfering substances was further evaluated, such as reactive oxygen species (H_2O_2, ClO^-, $ONOO^-$, and $^{\bullet}OH$), metal ions (Ca^{2+}, Fe^{3+}, Mg^{2+}, Zn^{2+}, Co^{2+}, K^+ and Cu^{2+}), iodine ion (I^-), amino acids (serine (Ser), cysteine (Cys), glutamate (Glu), arginine (Arg), tyrosine (Tyr), leucine (Leu), alanine (Ala), aspartate (Asp)), glutathione (GSH), nicotinamide adenine dinucleotide (NADH), glucose, and proteases (chymotrypsin, nitroreductase, leucine aminopeptidase (LAP), tyrosinase, β-galactosidase and carboxylesterase) (Fig. S11 in Supporting information). To our delight, the fluorescence of probe CES-Lyso at 595 nm could be markedly triggered only by CES, while the others showed negligible fluorescence changes.

To further validate the CES-dependent selective response, three representative carboxylesterase inhibitors bis-*p*-nitrophenyl phosphate (BNPP), 4-(2-aminoethyl)benzenesulfonyl fluoride hydrochloride (AEBSF) and loperamide (LPA) [16] were used to run the

inhibition test. As shown in Fig. S12 (Supporting information), all of these three inhibitors could restrict the fluorescence emission by suppressing the hydrolysis of CES-Lyso in a dose-depended manner, which suggested that CES-Lyso hydrolysis was catalyzed selectively by CES. While their efficiencies are different, LPA shows the strongest inhibition effect among these inhibitors under the same concentrations, indicating the high-throughput screening capability of CES-Lyso for hCE2 inhibitors. Moreover, a panel of commercially available subtypes of human carboxylesterases with close enzyme activity including CES1b, CES1c and CES2 were purchased to investigate their interactions and fluorescent responses with CES-Lyso (Fig. S13 in Supporting information). Unexpectedly, after incubation with each of the subtype enzyme, the probe showed fluorescence response quickly. The higher the enzyme concentration, the more obvious the response. The above analysis brings insight that CES-Lyso is an appropriate common substrate to be used to broadly sense the activity of multi carboxylesterases, as a proof of concept, not only for animal origin, but also for human subtypes. Off note, the ESI-MS (electrospray ionization mass spectroscopy) analysis indicated the release of fluorophore **4** with catalysis of CES, displaying a peak at *m/z* 399 $[M]^+$ (Fig. S14 in Supporting information) and offering expected proofs for the plausible reaction mechanism depicted in Scheme 1. In order to further check the specificity of CES-Lyso toward CES, a molecular modelling study was performed by docking CES-Lyso to the CES active domain using the Surflex-dock module built in the Sybyl-X 1.1 program (Fig. S15 in Supporting information). The docking score expressed in $-\lg K_d$ used to evaluate the affinity between the ligand and receptor generated by the docking simulation for binding to CES is the weighted sum of the nonlinear functions of the exposed atomic vander Waals surface distances of the protein-ligand. Firstly, probe CES-Lyso was docked into the CES active center for docking-scoring simulations, the score was returned as 6.95, and the lowest binding energy was calculated as −284.15 kcal/mol, indicating strong binding affinity of CES-Lyso to CES and being in consistent with the experimental results. The molecular model (Fig. S15B) shows that the hydroxy groups at C2, C3 and C6 of the glycosyl form five H-bonds with residues Glu136, Arg140 and Asp30 of CES within 3 Å, which is responsible for the high affinity and hydrolysis activity. These results showed that CES-Lyso could work as a highly specific probe for CES.

The above excellent performance of the probe CES-Lyso encouraged us to explore the potential application of CES-Lyso to perceive the intracellular CES alteration in live cells under changed pathophysiological conditions by means of laser scanning confocal imaging. Primarily, the cytotoxic effect of CES-Lyso was performed *via* a credible MTT (3-(4,5-dimethylthiazol-2-yl)-2,5-diphenyltetrazolium bromide) assay [28] on two kinds of cells stemming from different sources, MCF-7 cells (human breast cancer cells) and 4T1 cells (a kind of mouse breast cancer cells) prior to the cell imaging. As shown in Fig. S16 (Supporting information), CES-Lyso brought about relatively weak cytotoxicity to both MCF-7 and 4T1 cells with a more than 80% viability of these two kinds of cells in the prescence of CES-Lyso with high concentration of 20 μmol/L for 24 h at 37 °C, indicating the good biocompatibility. Next, the confocal fluorescent imaging experiment of probe CES-Lyso was performed on live cells. The intracellular time-dependent fluorescent imaging evaluated every 15 min displayed that CES-Lyso could get into the live cells efficiently and the subsequent fluorescent response for monitoring real activity of CES could reach the equilibrium within 30 min (Fig. S17 in Supporting information). However, if MCF-7 cells pretreated with 100 μmol/L representative inhibitors AEBSF or BNPP for 5.5 h and then treated with CES-Lyso for 30 min, the red fluorescence signal intensity of MCF-7 cells would be suppressed significantly (Figs. S18A and S19A in Supporting information), whose changes were consistent with those by the corresponding flow cytometric assays (Figs. S18B and S19B in Supporting information) thus confirming the selective detecting ability of CES-Lyso to CES in complex physiological system.

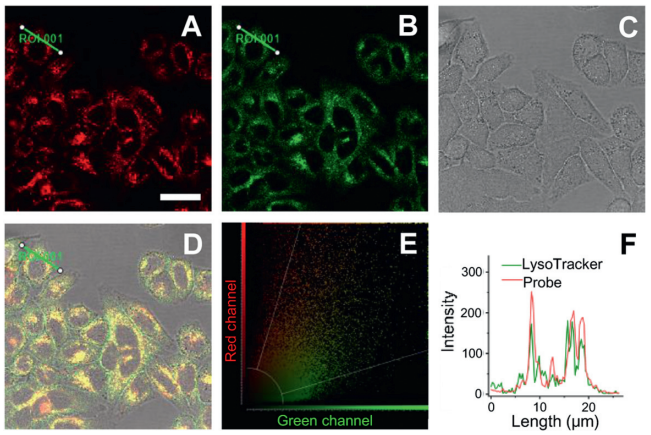

Fig. 2. Colocalization of CES-Lyso and LysoTracker®Green in MCF-7 cells. Cells were co-stained with CES-Lyso (10 μmol/L) and LysoTracker®Green (400 nmol/L) at 37 °C for 0.5 h. (A) Fluorescence image from CES-Lyso channel ($\lambda_{ex} = 561$ nm, $\lambda_{em} = 590$-700 nm). (B) Fluorescence image from LysoTracker®Green channel ($\lambda_{ex} = 458$, $\lambda_{em} = 470$–550 nm). (C) Corresponding DIC image. (D) Triple merged image of images A, B and C. (E) Fluorescence intensity correlation plot of CES-Lyso and LysoTracker®Green. (F) Intensity profile of the linear ROI 1 across the cell (green line in image D). Scale bar: 30 μmol/L.

We next tested the subcellular targeting property of CES-Lyso. The commercial co-staining dyes were a lysosomal tracker LysoTracker®Green, a mitochondrial tracker rhodamine 123, and a nuclear tracker Hoechst 33342. As presented in Fig. 2, the bright fluorescent regions of the co-stained parts within cells from the CES-Lyso channel (with denoted red pseudo color, Fig. 2A) overlap well with those from the LysoTracker®Green channel (green, Fig. 2B), with a relatively high Pearson's coefficient of 0.73 and an overlap coefficient of 0.81. It is noted that the yellow colour (Fig. 2D) formed by large area merging the above green fluorescence and red fluorescence verifies the nice co-staining, along with a consistent and coincident scatter plot (Fig. 2E). Besides, the change trends of the intensity profiles from the linear region of interest (ROI) across the MCF-7 cell are in close synchrony in both channels (Fig. 2F). Unlike the above, the co-staining test with CES-Lyso and rhodamine 123 (a commercial mitochondria-targeting dye) displays little overlapping effect with a poor Pearson's coefficient of 0.14 and weak overlap coefficient of 0.30 (Fig. S20 in Supporting information). Fig. S21 (Supporting information) showed that the fluorescence from nuclear targeting dye correlated weakly with that from CES-Lyso. The above findings suggest that CES-Lyso could target lysosome exclusively, which could serve as a useful tool for the evaluation of CES changes and regulation under lysosome stress and some lysosome-related diseases. This interesting result further indicates that the galactose subunit in some molecules tends to specifically deliver the molecules into lysosomes [29–32].

Inspired by the excellent performance of CES-Lyso in imaging the CES activity of MCF-7 cells, we next made an attempt to apply CES-Lyso to sense the fluorescence discrepancy of CES level in two different cancer cells MCF-7 and 4T1 which derived from human and mouse respectively. Both cells were treated with CES-Lyso under the same experimental conditions. Although emitted fluorescence of CES-Lyso in the two kinds of cells could be detected, there were obvious differences of their signal intensities. As shown in Fig. 3A, the red fluorescence of MCF-7 cell is much brighter than that of 4T1 cells. The data change trend is consistent with the flow cytometry analysis in Fig. 3B, which macroscopically reflects

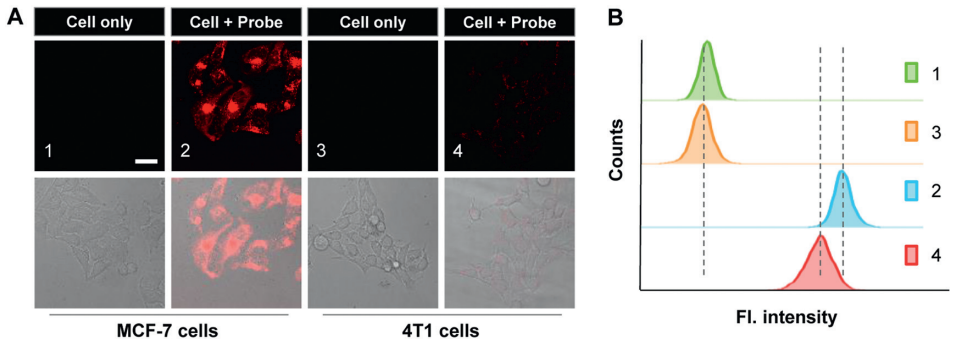

Fig. 3. The study of the effect of CES-Lyso on cancer cell homology research. (A) Confocal microscopy imaging of MCF-7 and 4T1 cells. Fluorescence signal collection from the cells covers 570-700 nm upon excitation wavelength at 561 nm. Representative scale bar: 30 μm. (B) Flow cytometry data from cells treated as the corresponding (A).

the change of fluorescence from the perspective of mega data. The reason for different fluorescence intensity might be owing to the different CES activity between the two cells. So our probe has the potential to be used to develop as a diagnostic kit for distinguishing human breast cancer cells from mouse derived breast cancer cells. To the best of our knowledge, it is the first exploration to use fluorescent probe to evidence that the CES activity is lower in mouse cancer 4T1 cells than in human MCF-7 cells.

The further application development of CES-Lyso aimed at the progress of anticancer drug treating cells. MCF-7 cells were cultured with medium containing 10 μmol/L 5′-deoxy-5-fluorouridine (an anticancer drug) for different time (0, 1, 2, 5 and 8 h) and then treated with CES-Lyso for 0.5 h. As shown in Fig. S22 (Supporting information), it is found that the fluorescence intensity has not changed significantly over time, indicating that the CES level would not be affected in the 5′-deoxy-5-fluorouridine treating process in a certain period of time.

To sum up, we present a new lysosomal-targeted fluorescent probe CES-Lyso to detect a variety of CESs with a red emission wavelength around 600 nm, good selectivity and low detection limit rapidly. It has the ability to sense the intracellular CES alteration *via* fluorescence imaging, which is applied to distinguish different derived cancer cells and monitor CES activity in the anticancer drug treatment. Therefore, CES-Lyso could serve as a highly turn-on fluorescent probe for elucidating the role of lysosomal CES in living cells and for exploring its associated biofunctions in drug discovery and disease diagnosis.

Declaration of competing interest

The authors declare that they have no competing interests.

Acknowledgments

We are grateful for the financial support from the National Natural Science Foundation of China (No. 21705120), the Technology Support Project of Shandong Province Higher Educational Youth Innovation (No. 2019KJM008), the Natural Science Foundation of Shandong Province, China (No. ZR2017LB016), the Project of Shandong Province Higher Educational Science and Technology Program (No. J17KB074).

Supplementary materials

Supplementary material associated with this article can be found, in the online version, at doi:10.1016/j.cclet.2022.01.087.

References

[1] M. Li, C. Zhai, S. Wang, et al., RSC Adv. 9 (2019) 40689–40693.
[2] A. Jiang, G. Chen, J. Xu, et al., Chem. Commun. 55 (2019) 11358–11361.
[3] Z. Tian, L. Ding, K. Li, et al., Anal. Chem. 91 (2019) 5638–5645.
[4] B. Shen, X. Zhang, J. Dai, et al., J. Hazard. Mater. 407 (2021) 124342.
[5] J. Dai, Y. Hou, J. Wu, et al., ChemistrySelect 5 (2020) 11185–11196.
[6] J. Kan, X. Zhou, Y. Sun, et al., Chin. Chem. Lett. 32 (2021) 3066–3070.
[7] C. Zhang, H. Xie, T. Zhan, et al., Chem. Commun. 55 (2019) 9444–9447.
[8] H.Y. Li, J.F. Chang, W.X. Lyu, et al., Chin. J. Anal. Chem. 48 (2020) 1325–1333.
[9] H. Li, H. Lin, W. Lv, et al., Biosens. Bioelectron. 165 (2020) 112336.
[10] S. Wang, B. Zhu, B. Wang, et al., Chin. Chem. Lett. 32 (2021) 1795–1798.
[11] H. Chu, L. Yang, L. Yu, et al., Coord. Chem. Rev. 449 (2021) 214208.
[12] S.D. Kodani, M. Barthélemy, S.G. Kamita, et al., Anal. Biochem. 539 (2017) 81–89.
[13] C. Ma, J. Wu, W. Sun, et al., Sens. Actuators B: Chem. 325 (2020) 128798.
[14] B. Shen, C. Ma, Y. Ji, et al., ACS Appl. Mater. Interfaces 13 (2021) 8718–8726.
[15] X.Y. Zhang, T.T. Liu, J.H. Liang, et al., J. Mater. Chem. B 9 (2021) 2457–2461.
[16] Y. Wang, F. Yu, X. Luo, et al., Chem. Commun. 56 (2020) 4412–4415.
[17] S.J. Park, Y.J. Kim, J.S. Kang, et al., Anal. Chem. 90 (2018) 9465–9471.
[18] A. Singh, M. Gao, M.W. Beck, et al., RSC Med. Chem. 12 (2021) 1142–1153.
[19] H. Zhou, J. Tang, J. Zhang, et al., J. Mater. Chem. B 7 (2019) 2989–2996.
[20] S. Samanta, S. Halder, G. Das, et al., Anal. Chem. 90 (2018) 7561–7568.
[21] B. Chen, S. Mao, Y. Sun, et al., Chem. Commun. 57 (2021) 4376–4379.
[22] B. Chen, C. Li, J. Zhang, et al., Chem. Commun. 55 (2019) 7410–7413.
[23] Z. Chai, D. Liu, X. Li, et al., Chem. Commun. 57 (2021) 5063–5066.
[24] Y. Lu, J. Xu, Z. Jia, et al., Chin. Chem. Lett. 33 (2022) 1589–1594.
[25] X. Chai, W. Zhu, Q. Meng, et al., Chin. Chem. Lett. 32 (2021) 210–213.
[26] D. Bu, Y. Wang, N. Wu, et al., Chin. Chem. Lett. 32 (2021) 1799–1802.
[27] G. Li, J. Wang, D. Li, et al., Chin. Chem. Lett. 32 (2021) 1527–1531.
[28] W.Y. Guo, Y.X. Fu, S.Y. Liu, et al., Anal. Chem. 93 (2021) 7079–7085.
[29] Y.H. Lee, N. Park, Y.B. Park, et al., Chem. Commun. 50 (2014) 3197–3200.
[30] A. Sharma, E.J. Kim, H. Shi, et al., Biomaterials 155 (2018) 145–151.
[31] H. Lee, S. Uhm, J.W. Shin, et al., Chem. Asian J. 10 (2015) 2695–2700.
[32] S. Dongbang, H.M. Jeon, M.H. Lee, et al., RSC Adv. 4 (2014) 18744–18748.